Geophys. J. Int. (2005) **163,** 689–697 doi: 10.1111/j.1365-246X.2005.02774.x

Studies on 'precarious rocks' in the epicentral area of the AD 1356 Basle earthquake, Switzerland

Peter Schürch[1] and Arnfried Becker[2]

[1] *Cyklamenweg 7,* CH-8048 *Zürich, Switzerland. E-mail: peter@paddeln.ch*
[2] *Sonneggstrasse* 57, CH-8006 *Zürich, Switzerland*

Accepted 2005 August 4. Received 2005 June 15; in original form 2004 November 10

SUMMARY

For the first time precarious rocks have been analysed in the epicentral area of the AD 1356 Basle earthquake in northern Switzerland. Several cliff sites in flat-lying, thickly bedded Upper Jurassic coral limestones in the Jura Mountains were investigated. Seven blocks are regarded as precarious with respect to earthquake strong ground motions. The age of these precarious rocks could not be determined directly as for instance by radiometric dating methods; however, based on slope degradation processes it can be concluded that the formation of these blocks predates the AD 1356 Basle earthquake. The acceleration required to topple a precarious rock from its pedestal is estimated using geometrical data for individual block sections and earthquake strong-motion records from stations on rock sites in the European Strong-Motion Database as input data for the computer program ROCKING V1.0 from the Seismological Laboratory, University of Nevada, Reno. The calculations indicate that toppling of a precarious rock largely depends on earthquake strength but also on the frequency spectrum of the signal. Although most investigated precarious rocks are surprisingly stable for ground motions similar to those expected to have occurred during the AD 1356 Basle earthquake, at least two blocks are clearly precariously balanced, with peak toppling accelerations lower than 0.3 g. Possible reasons why these blocks did not topple during the AD 1356 Basle earthquake include incomplete separation from their base, sliding of precarious rocks, their size, lower than assumed ground accelerations and/or duration of shaking.

Key words: AD 1356 Basle earthquake, peak ground acceleration, precarious rocks, seismic hazard assessment.

1 INTRODUCTION

Seismologically, northern Switzerland (Fig. 1) is well known for the AD 1356 Basle earthquake. It was the strongest historical earthquake north of the Alps, which was felt in northern and central Switzerland, eastern France, most parts of SW Germany and as far as Paris and Prague (Mayer-Rosa & Cadiot 1979; Meyer *et al.* 1994; Swiss Seismological Service, http://www.seismo.ethz.ch). In the Basle region it caused devastation in the city and villages and destruction of many strongholds (Fig. 1). Written documents and archaeological evidence allow an estimate of the earthquake intensities (MSK and EMS-98) in the epicentral area south of Basle of between VIII and IX–X (Fig. 1).

The historical record indicates an elevated level of seismicity in northern Switzerland, which stimulated the palaeoseismological research in the Basle region (Becker *et al.* 2005) aimed at deciphering the history of strong earthquakes in the region for the postglacial period. However, it was also intended to complete the archaeological and historical information about the AD 1356 Basle earthquake. The palaeoseismological results could show that the Basle-Reinach Fault south of Basle (Fig. 1) is the seismogenic fault for the AD 1356 Basle earthquake (Ferry *et al.* 2005; Meghraoui *et al.* 2001). In addition it was found that the Basle earthquake damaged speleothems in caves (Lemeille *et al.* 1999), triggered numerous rock falls (Becker & Davenport 2003) and caused soft-sediment deformation in lake deposits up to 60 km from the epicentre (Monecke *et al.* 2004).

During field investigations of cliff sites for the rockfall study (Becker & Davenport 2003) some blocks could be seen *in situ* along the edges of tall cliffs, which appeared to be instable with respect to high values of strong ground motion (Fig. 2). They might be 'precarious rocks' or 'semi-precarious rocks' that could be toppled by ground motions with peak accelerations between 0.1–0.3 g and 0.3–0.5 g, respectively (Brune 1996, 1999). Surprisingly, all of these 'precarious rocks' are located only 4–6 km from the Basle-Reinach Fault (Fig. 1), the seismogenic fault for the AD 1356 Basle earthquake. This raises two questions which are addressed in this study:

(1) what is the age of the blocks and

(2) assuming that they were already in place at the time of the AD 1356 Basle earthquake, what are the toppling accelerations for these blocks?

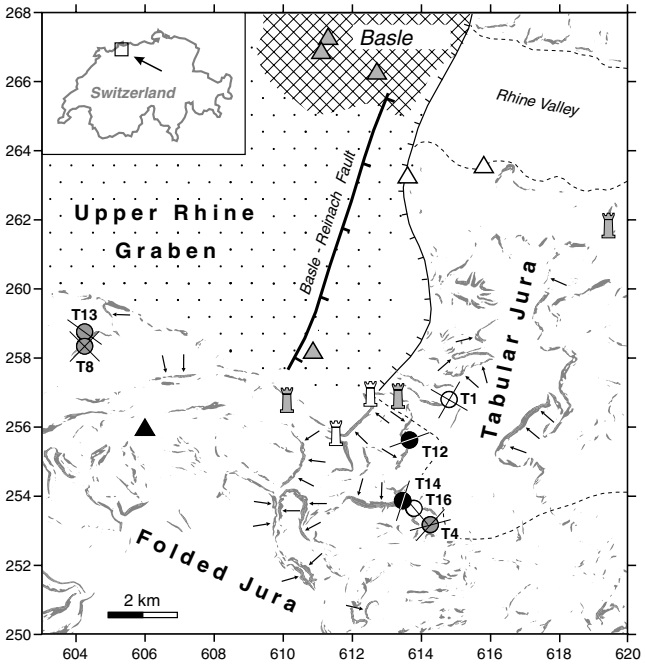

Figure 1. Setting of the study area in the Folded and Tabular Jura Mountains south of Basle in northern Switzerland. Grey areas indicate slopes dipping with $>30°$, small arrows mark cliff sites investigated in this study. The Basle-Reinach Fault is shown by a jagged bold line, the main Eastern Border Fault of the Upper Rhine Graben by a simple jagged line. Macroseismic intensities (EMS-98) for cities (triangles) and castles (towers) are IX–X (black), IX (grey) and VIII (white). Precarious rocks (circles) are distinguished as those, which are largely stable (white), semi-precarious in cases (grey) and precarious (black) with black lines indicating the section azimuths. Numbers along the border of the map refer to Swiss geographical coordinates (km).

The following study is motivated by the potential use of such blocks as natural strong-motion seismoscopes, as described by Brune (1996, 1999), to provide constraints on estimates of ground motion experienced during the AD 1356 Basle earthquake.

2 GEOLOGICAL SETTING

The study area south of Basle, Switzerland is situated in the Tabular and Folded Jura Mountains close to the southeastern end of the Upper Rhine Graben (Fig. 1). The Mesozoic sedimentary rocks in the Folded Jura and in the Tabular Jura consist of claystones and marls with intercalated limestones, some as thick as 100 m (Bitterli-Brunner & Fischer 1988). These limestones crop out as numerous cliff scarps (grey patches in Fig. 1). The most spectacular cliffs, reaching heights of up to 50 m, are those formed in the thick-bedded Upper Jurassic Rauracian limestones, which are underlain by Upper Jurassic Oxford marls. During several reconnaissance investigations most Rauracian limestone cliff sites in the epicentral area of the AD 1356 Basle earthquake could be analysed (arrows in Fig. 1) showing some spectacular precarious rocks (Fig. 2).

The Basle-Reinach Fault, the seismogenic fault for the AD 1356 Basle earthquake, appears to be a normal fault in the trench sites (Ferry *et al.* 2005; Meghraoui *et al.* 2001), with a possible minor sinistral strike-slip component. In the landscape it is clearly recognizable as a straight fault scarp between the northern front of the Folded Jura in the south and the outskirts of Basle in the north (Fig. 1). Tracing of the fault within the city of Basle was not yet possible and the southern surface continuation within the Folded Jura

Figure 2. Examples for precarious rocks in the Jura Mountains south of Basle: A Stüppen (T8), B Pelzmüli (T14).

is also unclear at the moment. Although the Basle-Reinach Fault shows traces of five major co-seismic ruptures during the post-glacial period with vertical displacements each between 0.5 and 1 m (Ferry *et al.* 2005), it is not the main Eastern Border Fault of the Upper Rhine Graben. The Basle-Reinach Fault instead is separated from the Eastern Border Fault (Fig. 1) by flat ground made up of up to 900-m-thick Tertiary and Quaternary deposits, with the topmost maximal 50 m consisting of gravels of the so-called 'Lower Terrace' (Niederterrasse).

3 ORIGIN AND AGE OF PRECARIOUSLY BALANCED ROCKS IN THE BASLE REGION

The Basle earthquake occurred 650 yr ago. The precarious rocks seen in the Jura Mountains are precariously or semi-precariously balanced rocks which can be used as natural 'low-resolution strong-motion seismoscopes' (Brune 1996) for the AD 1356 Basle earthquake only if they are older than 650 yr. Only in this case a shape and a position similar to the present one can be assumed for the situation 650 yr ago. Erosion, corrosion (dissolution) and, particularly, slope degradation are important processes generating precarious rocks in the Jura Mountains.

Fissures forming in the limestone behind the cliff faces that show orientations parallel to the trend of neighbouring valleys, can be considered tension cracks due to topographic relief perpendicular to the valley trend, partly reactivating pre-existing joints. The two most important cliff failure mechanisms, which have the potential to generate columns and slabs separated from the cliff face are toppling (Fig. 3a) and gliding (Fig. 3b). Toppling by outward movement of flat-lying Rauracian limestone slabs and columns is mainly caused by loss of lateral support and weakening of the underlying Oxford marls due to weathering in the valley ground. Also wedging by roots and ice can be important. In contrast, gliding of whole limestone cliff sections on marl occurs only when bedding dip exceeds *ca.* 10–15° to overcome the residual shear strength of the underlying weathered Oxford marls. The rate of degradation is also controlled by the degree of erosion at the cliff's foot; high erosion rates at the cliff's foot increases the rate of cliff failure. This is particularly true for the toppling case (Fig. 3a) which is a potentially stable situation with generally low degradation rates. In contrast, Fig. 3(b) shows a potentially instable configuration primarily controlled by bedding

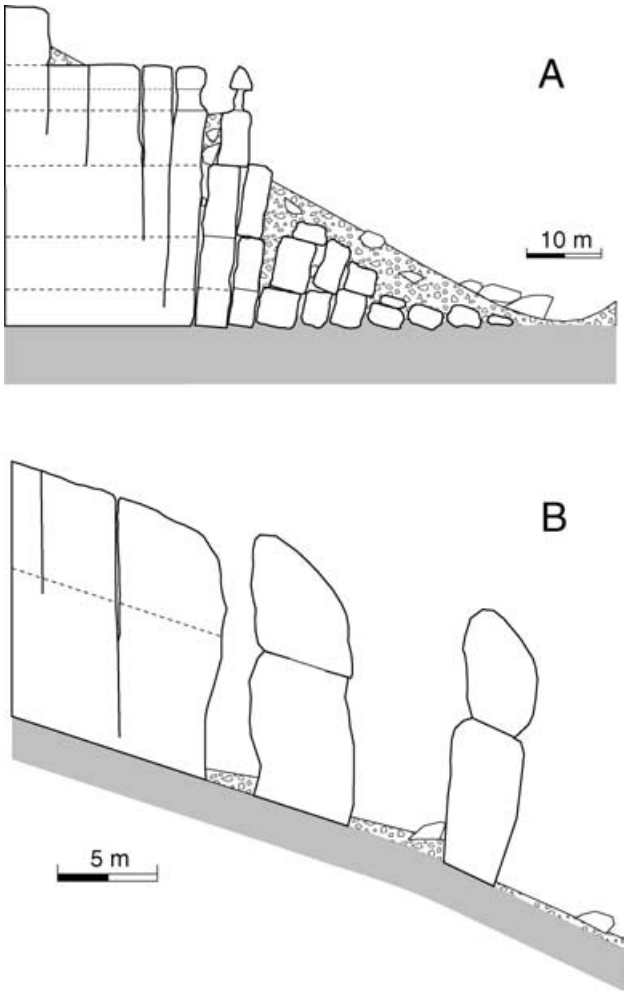

Figure 3. Two principle modes of cliff failure in the Upper Jurassic Rauracien limestones of the Jura Mountains south of Basle: (a) 'toppling' in flat-lying, (b) 'gliding' in at least 10–15° dipping beds.

dip and less by the erosion rate at the cliff's foot. Thus, it looks that the situation shown in Fig. 3(a) is more favourable for formation and preservation of precarious rocks because of lower degradation rates and because of the increased influence of weathering processes on the precarious rock formation. Indeed, all investigated precarious rocks were found in horizontal or flat-dipping Rauracian limestones.

Corrosion of limestone is particularly important in the intact rock mass before the mechanical separation of rock slabs and columns from the cliff face. The dissolution of limestone along fracture and bedding planes weakens the rock mass already long before slope degradation processes commence. Theoretically, rain water in bare karst (i.e. karst without soil at the surface) at 10°C and an annual precipitation of 1000 l m^{-2} (approx. the annual average for the southern Tabular Jura) can solve 62 g m^{-2} limestone, that is, causes 25 mm surface corrosion in 1000 yr, which is slightly higher than the actually measured 14–20 mm in 1000 yr (Bögli 1980; Delalieux *et al.* 2002; Stünzi 1994). The corrosion rate can be much higher in covered karst with soil on top of the limestone as long as the water is in contact with the CO_2-rich air in the soil. However, away from the earth surface the corrosion rate decreases significantly as soon as 80 per cent of the carbonate solubility is reached. Thus, formation of precarious rocks solely by dissolution of limestones would probably need several 1000 or even 10 000 yr.

Erosion is only active at the cliff's surface and is mainly related to frost weathering. Debris talus built-up by angular shards is widespread at various cliff sites, indicating the importance of frost weathering. However, quantifying frost weathering is not yet possible for the Rauracian limestones, only a comparison with the corrosion rate can be made in places. It appears that pure coral limestone is less sensitive to frost weathering than marly limestone. This is particularly true for marly limestone cropping out at cliff bases. Here, fracturing of the low-strength marly limestone due to high stresses at the cliff's foot and a slightly increased moisture content in the marly limestones provide ideal conditions for an efficient frost weathering. This process could generate notches at the cliff's foot, so-called abris, which even may cause cliff collapse. These observations also show that frost weathering in marly limestones can reach a much higher erosion rate than the combined effects of corrosion and frost weathering in pure coral limestones. In places with slightly different lithologies the combined effects of corrosion and frost weathering may further weaken the pedestal of precarious rocks (*cf.* Fig. 2a).

Direct age information for the precarious rocks is not yet available. Neither has rock varnish formed on the rock surfaces (Bell *et al.* 1998), nor do favourable lichens grow on carbonatic rocks, which could be used for dating purposes (Becker & Davenport 2003; Bull 1996). Solely, the ^{36}Cl-method seems to be promising based on first test measurements in Rauracian limestones (Ivy-Ochs, private communication, 2001); however, dates are not yet available for precarious rocks. Thus, for the moment, the age of precarious rock formation in the Jura Mountains south of Basle can only be estimated based on analogue examples from the literature. One example very close to the situation in the Jura Mountains is described by Schumm & Chorley (1964). The so-called Threatening Rock developed on 40-m-thick, flat-lying, wide-spaced jointed, thick-bedded sandstones on top of shales. It was separated by a fissure parallel to the cliff face and toppled by undermining of the cliff foot. The progressive opening of the fissure was monitored starting 5 yr before failure of Threatening Rock. This database led Schumm & Chorley (1964) to conclude that separation of Threatening Rock from the cliff face probably started about 2500 yr before its failure. Of course, a prediction based on such a short observation interval is highly debatable, as can be shown for the opposite case, that is, forecasting of slope failures based on short-term observations (Zvelebil & Moser 2001). However, we think the date given by Schumm & Chorley (1964) is a lower age limit for the precarious rocks seen in flat-lying, thick-bedded Rauracian limestones in the Basle region. Based on the weathering profiles of some precarious rocks (*cf.* Fig. 2a) and the thick debris deposits at many cliff foots (Fig. 3a), which protect the cliff foot against erosion and support the rock cliff laterally, we think that the investigated precarious rocks are at least a few thousand years old and thus represent natural strong-motion seismoscopes for the AD 1356 Basle earthquake.

4 PRECARIOUS ROCK METHODOLOGY

4.1 Field reconnaissance and measurements

In a field survey during the winter season several of the major cliff sites were investigated in the Jura Mountains south of Basle (Fig. 1). At different sites 17 blocks could be found which look instable. However, it was decided to include in this study only these seven blocks

Table 1. Location of the investigated precarious blocks, their volumes, masses, geometrical parameters for the calculation of the toppling accelerations and the section azimuths (Fig. 4).

Block	Swiss geogr. coordinates	Volume (m^3)	Mass (kg)	R_1 (cm)	R_2 (cm)	α_1 (°)	α_2 (°)	δ (°)	Section azimuth (N°...°E)
Tüfleten T1-1	614800	3.44	9100	108	130	37	41	4	30
Tüfleten T1-2	256800			107	121	41	33	9	120
Fulnau T4-1	614250	2.96	7800	159	152	18	16	3	75
Fulnau T4-2	253175			161	153	22	14	1	44
Stüppen T8-1	604250	2.40	6400	90	103	28	23	11	135
Stüppen T8-2	258350			120	90	34	27	10	48
Falkenflue T12	613650	2.05	5400	122	115	21	6	0	70
	255625								
St. Annafeld T13	604250	1.31	3500	92	92	21	21	0	126
	258750								
Pelzmüli T14	613450	37.66	99 800	375	349	13	16	9	18
	253875								
Pelzmüli T16	613775	13.78	36 500	238	212	29	25	5	320
	253650								

(1) which are completely exposed and have no contact with surrounding blocks or the cliff face,

(2) which have a small seating compared to their height and

(3) which show clearly visible bedding planes suggesting the block is detached from its base.

The location of these blocks is shown in Fig. 1 and their positions in Swiss geographic coordinates are given in Table 1. The block geometry and the bedding plane dip were measured, occasionally with the assistance of mountain-climbers. Idealized line drawings of the blocks are shown in Fig. 4.

4.2 Data analysis

Following the 2-D analysis of the toppling problem given by Shi *et al.* (1996) it is assumed (1) that the rigid block resting on a pedestal is free to rotate about either of the two supporting points O_1 and O_2(Fig. 5) and (2) that no sliding occurs during the rocking motion between the block and the base. R_1 and R_2 measure the distances between the rocking points O_1 and O_2, respectively, and the centre of mass, α_1 and α_2 are the angles between R_1 and R_2, respectively, and the vertical, δ is the dip of the seating in the sectional plan. For the calculation of the centre of mass and the geometrical parameters

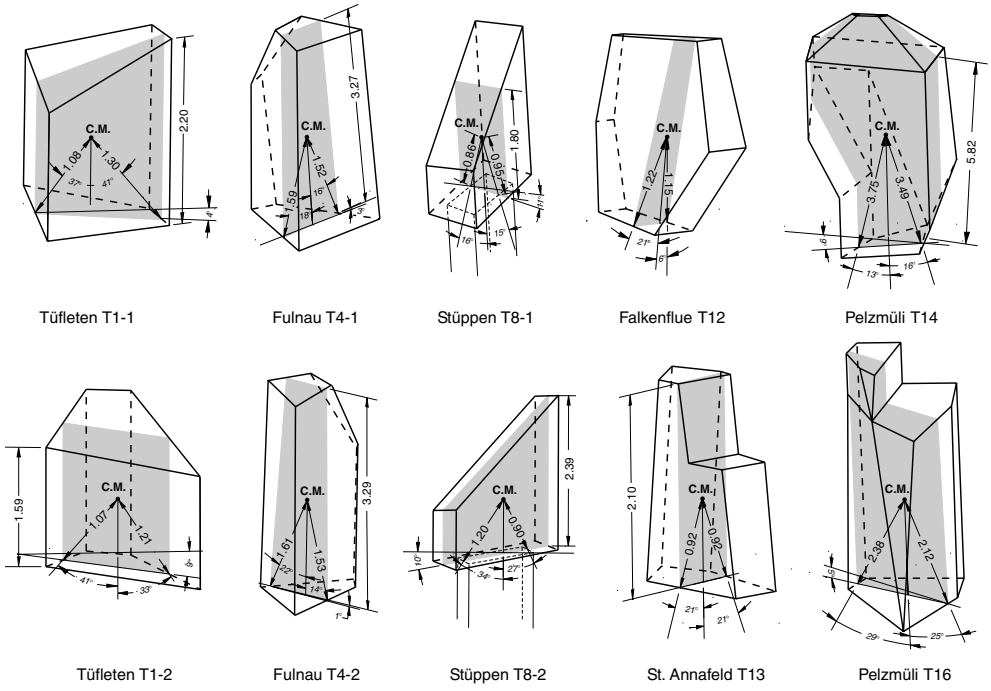

Figure 4. Details about the geometry of the investigated precarious rocks (T1–T16) with sections (grey) selected for the calculation of the toppling accelerations. Lengths are given in metres. C.M.: centre of mass.

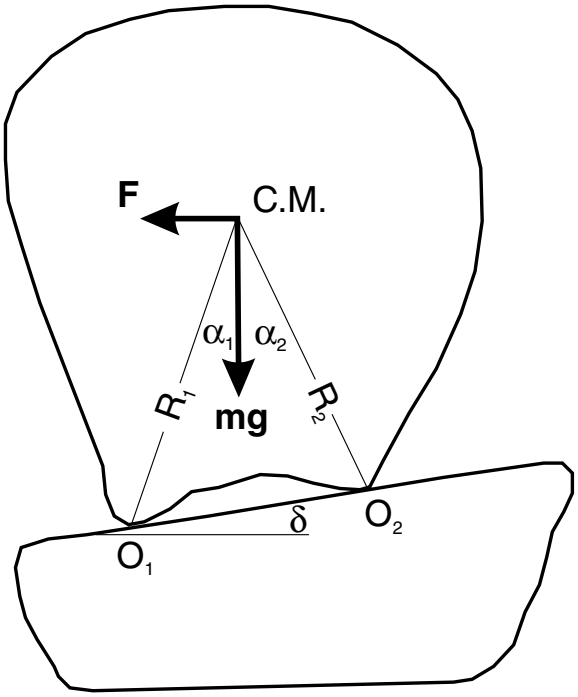

Figure 5. Summary of the geometrical input data for the calculation of the toppling accelerations: R_1, R_2 distances from the centre of mass (C.M.) and the supporting points O_1, O_2; α_1, α_2 angles between R_1, R_2, respectively, and the vertical; δ dip of the pedestal surface.

the AutoCAD-2002 program was used. The geometrical parameters are shown in Fig. 4 and summarized in Table 1 with the azimuths of the sectional planes given in the last column.

During earthquakes the horizontal components of ground motion play a dominant role in toppling of rocking blocks. For the determination of the horizontal peak toppling acceleration necessary to overturn a precariously balanced rock, the FORTRAN program ROCKING V.1.0 (von Seggern 2001) of the Nevada Seismological Laboratory was used. This program is based on the equation of motion of a rocking rigid block about supporting points O_1 and O_2 due to the accelerating motion of the foundation (Shi *et al.* 1996). No analytical solution exists except for simple block geometries and small angles. Thus, the equation is integrated numerically using a Runge-Kutta algorithm for given input values for the horizontal ($\bar{a}_x$ or $\bar{a}_y$) and vertical ground acceleration ($\bar{a}_z$) (von Seggern 2001). Details about the theoretical background are given in Shi *et al.* (1996), for the computation of the toppling accelerations in von Seggern (2001), and for experimental verification of the rocking theory in Shi *et al.* (1996), Anooshehpoor & Brune (2002) and Anooshehpoor *et al.* (2004).

Input data are: (1) geometrical parameters (Fig. 5) for the most favourable toppling sections, which are defined by the smallest angles α_1 or α_2 and the largest value for δ for a given geometry. These sections are shown in grey in Fig. 4 for the investigated blocks. In cases where the most favourable toppling direction was unclear, two sections were defined for calculations of blocks T1, T4 and T8 (Fig. 4). (2) Acceleration data were taken from the European Strong Motion Database (Ambraseys *et al.* 2001) using seismograms from stations on hard rock, which are as close as possible to the seismogenic fault and/or epicentre. Preferentially accelerograms were selected from shallow normal-faulting earthquakes with magnitudes Ms 6–7 (Table 2), that is, data close to the expected AD 1356 Basle earthquake based on macroseismical, archaeological and palaeoseismological evidence (Fäh *et al.* 2003; Ferry *et al.* 2005; Mayer-Rosa & Cadiot 1979).

4.3 Results

Table 3 lists the toppling accelerations for the most susceptible rock sections (Fig. 4, Table 1) for the different earthquake signals recorded at the stations listed in Table 2. The lowest toppling accelerations in Table 3 are shown in bold; asterisks mark the cases where no toppling at all occurred. Table 3 shows that some blocks are very stable with hardly any toppling for the applied signals, or if at all, then only for large peak ground accelerations >1 g. In these cases, sliding is much more likely than toppling failure. An ideal precariously balanced rock should be slim and tall, which is obviously not the case for the block Tüfleten T1-1/2 (Fig. 4) and also Pelzmüli T16 seems to be well founded on its broad seating. For Stüppen T8 (Table 1, Fig. 2a) two sections were analysed, although it should be clear in advance that section Stüppen T8-1 is the less stable one. Both sections are relatively stable against toppling and only for a few signals toppling would have occurred close to accelerations around 0.5 g. This example shows that if the distance between the centre of mass and the pedestal is small, that is, the angles α_1 and α_2 are large, the block is very stable against toppling. Falkenflue T12 comes close to an ideal slim and tall precariously balanced rock with a small seating. This block topples for all applied seismic signals frequently toppling accelerations as low as 200 to 500 cm s^{-2}. Also

Table 2. Input signals for the calculation of toppling accelerations from seismic stations on rock taken from the European Strong-Motion Database (Ambraseys *et al.* 2001). WF ID waveform identity, EQ name of earthquake, HY focal depth, FM focal mechanism, ED epicentral distance, FD fault distance.

WF ID	EQ	Date	HY (km)	Ms	FM	Station	ED (km)	FD (km)	$\bar{a}_{\text{horiz}}$ (m s^{-2})	$\bar{a}_{\text{vert}}$ (m s^{-2})
055	Friuli	1976/05/06	6	6.5	Thrust	Tolmezzo-Diga Ambiesta	27	6	3.499	2.623
158	Ardal	1977/04/06	10	6	Thrust	Naghan1	5	4	8.911	–
182	Tabas	1978/09/16	5	7.3	Thrust	Dayhook	11	11	3.317	1.709
198	Montenegro	1979/04/15	12	7	Thrust	Ulcinj-Hotel Albatros	21	9	2.200	2.077
242	Valnerina	1979/09/19	4	5.8	Normal	Bagnoli-Irpino	23	6	1.776	1.017
287	Campano Lucano	1980/11/23	16	6.9	Normal	Bagnoli-Irpino	23	6	1.776	1.017
290	Campano Lucano	1980/11/23	16	6.9	Normal	Sturno	32	14	3.166	2.308
292	Campano Lucano	1980/11/23	16	6.9	Normal	Auletta	25	10	0.588	0.344
363	Umbria	1984/04/29	7	5.6	Normal	Pietralunga	30	19	2.045	0.499
365	Lazio Abruzzo	1979/09/19	8	5.8	Normal	Atina	15	12	1.081	0.641
593	Umbro-Marchigian	1997/09/26	7	5.5	Normal	Nocera Umbra	13	13	4.613	1.592
763	Umbro-Marchigian	1997/09/26	7	5.5	Normal	Borgo-Cerreto Torre	23	17	1.831	1.013

Table 3. Results for the toppling acceleration for the different seismic input signals and the investigated precarious rock geometries. Marked in grey are those results where scaling factors >2 are applied to the signals. The boundaries for $\bar{a}$ in the lower section refer approximately to what Brune (1996) defined as semi-precariously (300–500 cm s^{-2}) and precariously balanced rocks (100–299 cm s^{-2}).

Signal	Toppling acceleration $\bar{a}$ (cm s^{-2}) for block section ...									
	T1-1	T1-2	T4-1	T4-2	T8-1	T8-2	T12	T13	T14	T16
055xz	*	*	1700	2000	1900	2600	300	1900	700	*
055yz	*	*	2100	1300	700	1000	200	1400	200	*
158xz	*	*	4500	2000	4000	8000	500	5000	1750	*
182xz	*	*	1200	1600	1100	1900	500	1700	600	*
182yz	3500	3300	1500	1400	1200	1600	300	1800	300	3300
198xz	*	*	800	800	750	1650	250	950	400	1600
198yz	2000	1800	700	**500**	800	1100	**200**	700	300	1150
242xz	*	*	*	*	1450	*	300	*	400	*
242yz	*	*	1100	*	1300	2000	500	1500	600	*
287xz	*	*	**450**	550	**500**	950	300	**500**	300	*
287yz	1400	1400	500	700	**500**	950	250	600	**150**	1350
290xz	**1200**	**1100**	600	**500**	600	**800**	**200**	600	300	**1100**
290yz	2300	2200	500	600	800	1600	**200**	700	200	1300
292xz	*	*	*	*	*	*	300	*	420	*
292yz	*	*	*	*	*	*	280	*	380	*
363xz	*	*	*	*	*	*	750	*	600	*
363yz	*	*	*	*	*	*	600	*	600	*
365xz	*	*	*	*	*	*	425	*	500	*
365yz	*	*	*	*	*	*	650	*	950	*
593xz	*	*	*	4200	4100	*	1200	*	1800	*
593yz	*	*	*	*	*	*	1100	*	1500	*
763xz	*	*	*	*	*	*	950	*	*	*
763yz	*	*	*	*	*	*	1250	*	1350	*
$\bar{a}$ (cm s^{-2})	Number of toppling events out of a total of 23									
>500	5	5	9	10	12	12	7	11	10	6
300–500	0	0	3	2	2	0	9	1	9	0
100–299	0	0	0	0	0	0	7	0	3	0

Pelzmüli T14 (Figs 2b and 4) is very instable with the lowest toppling acceleration at 150 cm s^{-2}. The high toppling acceleration values for the signals 593 and 763 may indicate that these earthquakes are too weak or shaking did not last long enough to cause toppling even of the most susceptible blocks. Whether a precarious rock topples depends strongly on the frequency spectrum of the seismic signal as well as the duration of shaking and not only on the earthquake strength. Fig. 6 illustrates the results given in Table 3 by drawing the probability of toppling versus toppling acceleration for the different earthquake signals and the different block sections. It illustrates that Tüfleten T1-1/2 are very stable showing only five toppling events (of 23) for accelerations >1 g. In contrast, toppling accelerations for Falkenflue T12 and Pelzmüli T14 are concentrated below 1g with a high probability of occurrence as low as 0.2 g. Stability of other blocks is between these extreme cases and the blocks potentially fail for horizontal accelerations between 0.5 to 1.0 g for certain ground motions.

5 DISCUSSION

Reconnaissance of several cliff sites (Fig. 1) in the epicentral area of the AD 1356 Basle earthquake supplied 17 'precarious rocks', of which seven were regarded as possibly instable during strong ground motion. From these only two (T12 and T14) are precariously and two (or three) further blocks are possibly semi-precariously balanced rocks following the definition by Brune (1996, 1999). We are aware of the small database and, thus, do not want to over-interpret our observations. Here, we only discuss the question why at all precariously balanced rocks can be found in the epicentral area of the Basle earthquake only 4–6 km from the Basle-Reinach Fault.

One reason why the blocks are still standing could be that they are not fully separated from their base, they are still—at least partly—'welded' to their pedestals. This assumption may be true for blocks T8 (Fig. 2a) and possibly for T4 and T12, but most unlikely for T14 (Fig. 2b). For values $\alpha > 25^\circ$ and dips $\delta \geq 10^\circ$ sliding of the rocks during strong shaking may occur, which dampens rocking motions and could prevent blocks from toppling (Anooshehpoor *et al.* 2004). This is a possible reason why T14 did not topple; however, sliding occurs only on a very smooth surface which is generally not the case for rock surfaces in a natural environment. Also the size of the precarious rock may have an influence on the toppling behaviour, particularly in the epicentral region, because larger blocks are more sensitive to the low-frequency components of ground motion compared to smaller blocks (Anooshehpoor *et al.* 2004).

Topography effects on the behaviour of precarious rocks during strong ground motions are ambivalent and by far not understood (Anderson & Brune 1999). On one hand, precarious rocks are on the top or at margins of cliffs, which could cause amplification (Geli *et al.* 1988). On the other hand, bedrock tends to cause smaller amplifications (Anderson & Brune 1999). Combined, the two effects may cancel each other resulting in an average behaviour. However, if the combined effect is higher than the average, that is, topography amplifies ground motion, the Basle earthquake should have been weaker although the effect on the investigate sites with precarious rocks was stronger.

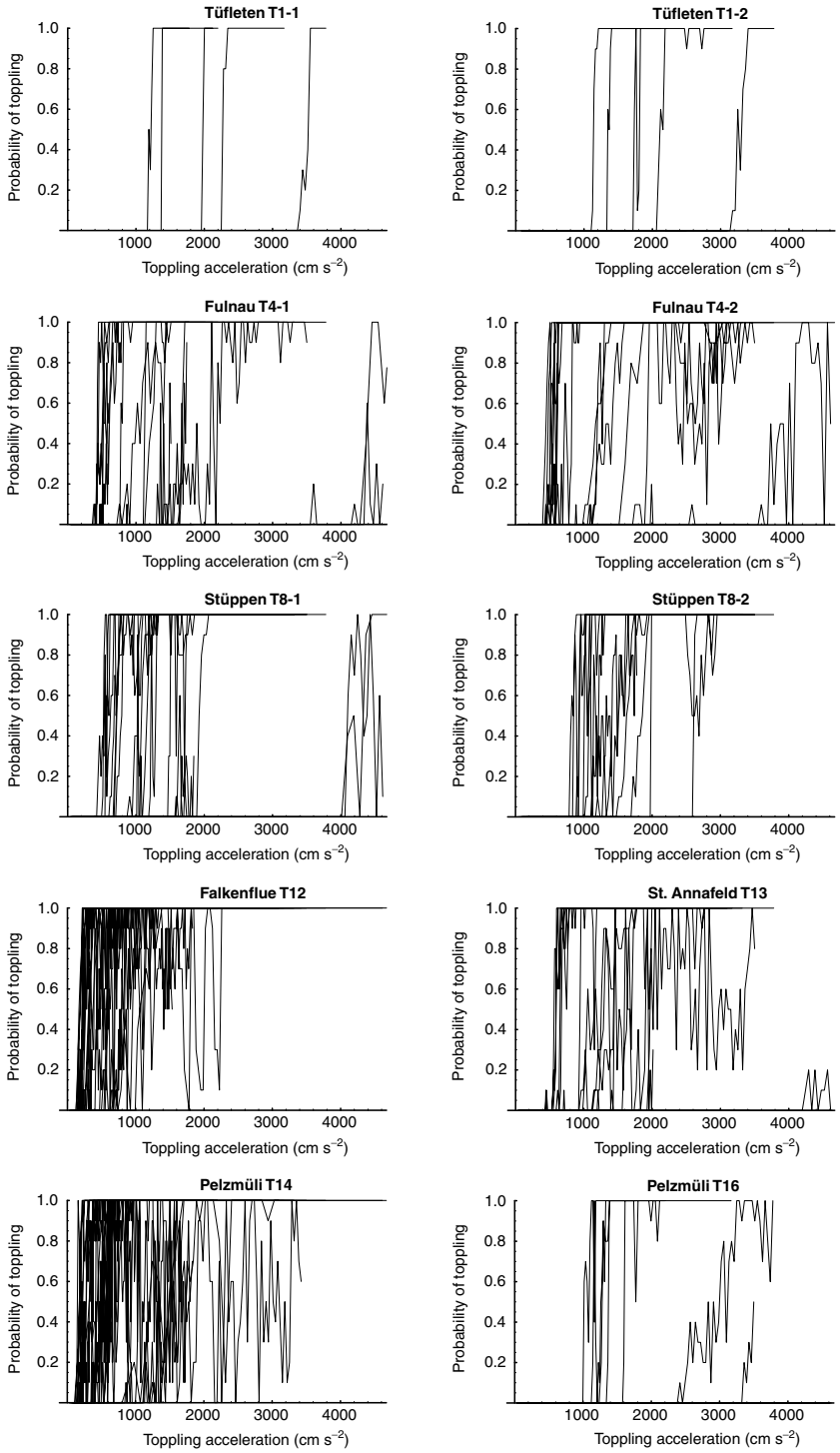

Figure 6. Diagrams showing the probability of toppling versus toppling acceleration for the different precarious rock sections (T1-1 to T16) for 23 applied seismic input signals as shown in Table 2.

Brune & Whitney (2000) concluded that earthquakes with intensities VII MM would probably have toppled most near-source precarious rocks, those with VIII MM would have toppled all. If it is assumed that toppling acceleration refers to the approximate peak ground acceleration (Brune & Whitney 2000), the toppling accelerations for the precarious rocks in the Basle region could be compared with peak ground accelerations expected for the AD 1356 Basle earthquake. With intensities VIII to IX–X MSK and a magnitude M_w 6.5 (Ferry *et al.* 2005) for the AD 1356 Basle earthquake, maximum horizontal peak ground acceleration could be as low as 360–460 cm s^{-2} at the investigation sites about 4–6 km from the seismogenic fault (Ambraseys *et al.* 1996). Lacave *et al.* (2004) estimated the peak ground acceleration for the Basle earthquake in a near-surface cave 5 km from the seismogenic fault with 1030 cm s^{-2} to explain the complete breaking of a group of stalactites. Although this value is still within the 1σ standard deviation

range of Ambraseys *et al.* (1996) attenuation equations this peak ground acceleration should have caused toppling of almost all precarious rocks investigated in this study (Fig. 6) and, certainly, for the precarious rocks T12 and T14. Considering only those signals that have been scaled-up by a factor of less than 2 (Table 3), toppling of the investigated precarious blocks should have occurred for peak ground accelerations between 200 and 600 cm s^{-2}. This range of maximum past peak ground accelerations would be compatible with a maximum magnitude M_w for the Basle earthquake in the range between *ca*. 5 and 7. However, signals used for calculation of toppling acceleration giving magnitude estimates $M_w < 6.0$ seem not to be compatible with the AD 1356 Basle earthquake palaeoseismic evidence from trench sites (Ferry *et al.* 2005), rockfalls (Becker & Davenport 2003) and damage of speleothems (Lemeille *et al.* 1999).

Brune (1996, 1999) concluded precariously balanced rocks do not exist in the close vicinity of seismically active faults like the San Andreas Fault. In the Mojave section of the San Andreas Fault no precarious rock was found within 14 km. Recently Brune (2003) described just such occurrences as close as 2–7 km from active faults with known historical earthquakes. These observations could be associated with low ground accelerations in the footwall of normal faults (Brune & Anooshehpoor 1999; Oglesby *et al.* 1998) and stepover regions along transtensional strike-slip faults (Brune 2003). Low ground accelerations from the Basle-Reinach fault embedded in an extending region of the southernmost Upper Rhine Graben with thick deposits of soft sediments in the surroundings may also explain that some of the precarious rocks in the close distance did not topple during the AD 1356 Basle earthquake. However, currently the database is too small to further elaborate such a model for the Basle region. As has been shown recently by near-source strong-motion data from the Chichi, Izmit and Denali earthquakes peak ground accelerations can be spatially highly variable and much lower than expected from published attenuation curves (Anooshehpoor *et al.* 2004) even in cases without any particular geological boundary conditions.

This study is the first attempt to apply the precarious rock methodology in the epicentral area of the AD 1356 Basle earthquake, an area with known high seismic energy release in Switzerland. Although several aspects deserve further investigations, such as effect of precarious rock size, possible sliding of precarious rocks, non-ideal contact surfaces between precarious rock and pedestal, and duration of input motion (Anooshehpoor *et al.* 2004), the method has the potential to directly indicate past ground shaking. This information can be used to complete the palaeoseismic information about pre-historical earthquakes and historical shocks, which are only weakly documented. The method can supply a significant contribution for the seismic hazard assessment in the Basle region where numerous cliff sites (Fig. 1) are still awaiting further investigations.

ACKNOWLEDGMENTS

The project was funded by the Swiss National Science Foundation (SNF) and the Federal Institute of Technology (ETH) Zürich in the frame of the former PALEOSEIS Project at the Geophysical Institute, Professor Dr D. Giardini. From the Seismological Laboratory, University of Nevada, Reno, we gratefully acknowledge James N. Brune and Abdolrasool Anooshehpoor for a copy of the computer program ROCKING and Matt Purvance for his patience in answering questions concerning the computer program. Finally we would like to acknowledge our former colleagues from ETH Donat Fäh for his help with the selection of seismic signals and discussions, and Jochen Braunmiller for his help to install the computer program and a critical review of the text as well as Patrick Müller and Thomas Michlmayr for the measurements of blocks in difficult positions.

REFERENCES

Ambraseys, N.N., Simpson, K.A. & Bommer, J.J., 1996. Prediction of horizontal response spectra in Europe, *Earthquake Eng. Struct. Dyn.,* **25,** 371–400.

Ambraseys, N., Smit, P., Sigbjörnsson, R., Suhadolc, P. & Margaris, B., 2001. Internet-Site for European Strong Motion Data, http://www.isesd.cv.ic.ac.uk

Anderson, J.G. & Brune, J.N., 1999. Methodology for using Precarious Rocks in Nevada to test seismic hazard models, *Bull. seism. Soc. Am.,* **89**(2), 456–467.

Anooshehpoor, A. & Brune, J.N., 2002. Verification of precarious rock methodology using shake table tests of rock models, *Soil Dyn. Earthquake Eng.,* **22,** 917–922.

Anooshehpoor, A., Brune, J.N. & Zeng, Y., 2004. Methodology for obtaining constraints on ground motion from Precariously Balanced Rocks, *Bull. seism. Soc. Am.,* **94**(1), 285–303.

Becker, A. & Davenport, C.A., 2003. Rockfalls triggered by the AD 1356 Basle earthquake, *Terra Nova,* **15,** 258–264.

Becker, A., Ferry, M., Monecke, K., Schnellmann, M. & Giardini, D., 2005. Multiarchive paleoseismic record of late Pleistocene and Holocene strong earthquakes in Switzerland, *Tectonophysics*, **400,** 153–177.

Bell, J.W., Brune, J.N., Liu, T., Zreda, M. & Yount, J.C., 1998. Dating precariously balanced rocks in seismically active parts of California and Nevada. *Geology,* **26**(6), 495–498.

Bitterli-Brunner, P. & Fischer, H., 1988. Erläuterungen zum Geologischen Atlas der Schweiz 1:25000, Blatt 1067 Arlesheim, 66 pp., Landeshydrologie und -geologie.

Bögli, A., 1980. *Karst hydrology and physical speleology*, Berlin, Springer, 284 pp.

Brune, J.N., 1996. Precariously Balanced Rocks and ground-motion maps for southern California, *Bull. seism. Soc. Am.,* **86**(1), 43–54.

Brune, J.N., 1999. Precarious rocks along the Mojave section of the San Andreas Fault, California: Constraints on ground motion from great earthquakes, *Seism. Res. Letters,* **70**(1), 29–33.

Brune, J.N., 2003. Precarious rock evidence for low near-source accelerations for trans-tensional strike-slip earthquakes, *Phys. Earth planet. Inter.,* **137,** 229–239.

Brune, J.N. & Anooshehpoor, A., 1999. Dynamic geometrical effects on strong ground motion in a normal fault model, *J. geophys. Res.,* **104**(B1), 809–815.

Brune, J.N. & Whitney, J.W., 2000. Precarious rocks and seismic shaking at Yucca Mountain, Nevada, US Geological Survey Digital Data Series 058, M, 1–19.

Bull, W.B., 1996. Dating San Andreas fault earthquakes with lichenometry. *Geology,* **24**(2), 111–114.

Delalieux, F., Cardell-Fernandez, C., Torfs, K., Vleugels, G. & van Grieken, R., 2002. Damage functions and mechanism equations derived from limestone weathering in field exposure. *Water, Air and Soil Pollution,* **139,** 75–94.

Fäh, D. et al, 2003. Earthquake catalogue of Switzerland (ECOS) and the related macroseismic database. *Eclogae geol. Helv.,* **96**(1), 219–236.

Ferry, M., Meghraoui, M., Delouis, B. & Giardini, D., 2005. Evidence for Holocene paleoseismicity along the Basle-Reinach active normal fault (Switzerland): a Seismic Source for the 1356 Earthquake in the Upper Rhine Graben, *Geophys. J. Int.,* **160,** 554–572.

Geli, L., Bard, P.-Y. & Jullien, B., 1988. The effect of topography on earthquake ground motion: a review and new results, *Bull. seism. Soc. Am.,* **78**(1), 42–63.

Lacave, C., Koller, M.G. & Egozcue, J.J., 2004. What can be concluded about seismic history from broken and unbroken speleothems?, *J. Earthquake Eng.,* **8**(3), 431–455.

Lemeille, F., Cushing, M.E., Carbon, D., Grellet, B., Bitterli, T., Fléhoc, C. & Innocent, C., 1999. Co-seismic ruptures and deformations recorded by

speleothems in the epicentral zone of the Basel earthquake, *Geodinamica Acta,* **12**(3–4), 179–191.

Mayer-Rosa, D. & Cadiot, B., 1979. A review of the 1356 Basel earthquake, *Tectonophysics,* **53,** 325–333.

Meghraoui, M., Delouis, B., Ferry, M., Giardini, D., Huggenberger, P., Spottke, I. & Granet, M., 2001. Active normal faulting in the Upper Rhine Graben and paleoseismic identification of the 1356 Basel earthquake, *Science,* **293,** 2070–2073.

Meyer, B., Lacassin, R., Brulhet, J. & Mouroux, B., 1994. The Basel 1356 earthquake: which fault produced it?, *TerraNova,* **6,** 54–63.

Monecke, K., Anselmetti, F., Becker, A., Sturm, M. & Giardini, D., 2004. Signature of historical earthquakes in lake sediments in Central Switzerland, *Tectonophysics,* **394,** 21–40.

Oglesby, D.D., Archuleta, R. & Nielsen, S.B., 1998. Earthquakes on dipping faults: the effects of broken symmetry, *Science,* **280** (15 May 1998), 1055–1059.

Schumm, S.A. & Chorley, R.J., 1964. The fall of threatening rock. *Am. J. Sci.,* **262,** 1041–1054.

Shi, B., Anooshehpoor, A., Zeng, Y. & Brune, J.N., 1996. Rocking and overturning of precariously balanced rocks by earthquakes, *Bull. seism. Soc. Am.,* **86**(5), 1364–1371.

Stünzi, H., 1994. Korrosion von Kalk. *AGS-Info,* **1/94,** 20–28.

von Seggern, D., 2001. Software management report, ROCKING v.1.0, Nevada Seismological Laboratory, 36 pp. (unpubl.)

Zvelebil, J. & Moser, M., 2001. Monitoring based time-prediction of rock falls: three case histories, *Phys. Chem. Earth,* **26**(2), 159–167.